Griffiths-McCoy singularities, Lee-Yang zeros, and the cavity method in a solvable diluted ferromagnet

C. Laumann,[1,2] A. Scardicchio,[1,2,3] and S. L. Sondhi[1,2]
[1]*Department of Physics, Joseph Henry Laboratories, Princeton University, Princeton, New Jersey 08544, USA*
[2]*Princeton Center for Theoretical Physics, Princeton University, Princeton, New Jersey 08544, USA*
[3]*MECENAS, Università Federico II di Napoli, Via Mezzocannone 8, I-80134 Napoli, Italy*
(Received 27 December 2007; revised manuscript received 17 April 2008; published 27 June 2008)

We study the diluted Ising ferromagnet on the Bethe lattice as a case study for the application of the cavity method to problems with Griffiths-McCoy singularities. Specifically, we are able to make much progress at infinite coupling where we compute, from the cavity method, the density of Lee-Yang zeros in the paramagnetic Griffiths region as well as the properties of the phase transition to the ferromagnet. This phase transition is itself of a Griffiths-McCoy character albeit with a power law distribution of cluster sizes.

DOI: 10.1103/PhysRevE.77.061139 PACS number(s): 05.70.Jk, 05.50.+q, 64.60.ah, 64.60.De

I. INTRODUCTION

The Bethe-Peierls or cavity method has a long history in statistical mechanics [1]. The application of this method to disordered systems has recently undergone a considerable revival, mainly in connection with the analysis of typical case complexity of random NP-complete [2] (i.e. difficult) optimization problems. This recent work has led to an improved understanding of the statistical mechanics of disordered systems—in particular to a formulation of the physics of replica symmetry breaking without resorting to replicas. Importantly, it has also led to an efficient class of algorithms, now known as survey propagation, for the optimization problems [3]. In addition, very recent work [4–6] has attempted to generalize the cavity method/belief propagation to disordered *quantum* systems, obtaining encouraging results.

The work alluded to above does not address one striking feature of the physics of disordered systems, namely the presence of Griffiths-McCoy (GM) singularities [7–9] in their thermodynamics in an applied field. While the form of these singularities can be readily determined from rough estimates of the statistics of the rare regions from which they emanate, their detailed extraction can be a tricky task due to their delicate nature, especially in classical systems [10]. Indeed, in field theoretic formulations they appear as nonperturbative (instanton) effects [11,12].

In this paper we consider the task of extracting these GM singularities from the cavity method. The method is exact on Bethe lattices and hence the functional recursion relation to which it gives rise must contain GM physics which exists already on these lattices. The challenge then, is to extract it by constructing the appropriate fixed point solution. To this end we study the particular case of a diluted ferromagnet on the Bethe lattice which has an extended GM region at low temperatures and large dilution. While the general, exact, determination of GM singularities everywhere in the phase diagram is a difficult problem, we are able to solve the problem in the infinite coupling limit made precise below. Here we can directly solve the cavity equations in a field and relate the solution to the statistics of clusters and to the density of Lee-Yang zeros commonly used to characterize GM effects. Further, in this limit the phase transition between the paramagnet and the ferromagnet is itself essentially of a GM character and its critical behavior, which we extract, can be viewed as an enhanced GM phenomenon.

The problem of the dilute Bethe lattice ferromagnet and of GM singularities has been considered before us [13,14] by different methods. As our interest is primarily in the development of the cavity method, we give a self-contained presentation in this paper from that viewpoint. We turn now to a more detailed enumeration of the contents of this paper.

II. MODEL AND ORGANIZATION

We consider the following disordered Ising Hamiltonian on the Bethe lattice with connectivity q:

$$\beta\mathcal{H}_{\epsilon} = -J\sum_{\langle ij\rangle}\epsilon_{ij}\sigma_i\sigma_j - H\sum_i \sigma_i, \tag{1}$$

where

$$\epsilon_{ij} = \begin{cases} 1 & \text{with probability } p \\ 0 & \text{with probability } 1-p. \end{cases}$$

The random couplings ϵ_{ij} indicate the presence or absence of a bond in the diluted Bethe lattice. For probability $p<p_c=1/(q-1)$ the lattice has no giant clusters and the density of large finite clusters decays exponentially. For $p>p_c$, giant clusters exist with finite density and at the percolation transition, $p=p_c$, the density of clusters of size n develops a long algebraic tail $W_n \sim n^{-5/2}$ (independent of q) [15]. We note that the dimensionless coupling constants J and H differ from the conventional magnetic exchange and field by factors of inverse temperature $\beta=1/T$. The limit $T\to 0$ with $J \gg H$ will be denoted as the $J=\infty$ limit.

In Sec. III, we provide a guided tour of the well-known phase diagram of this model from the point of view of the cavity method. We then establish the critical behavior at the phase transitions using a set of recursion relations for the moments of the cavity field distribution. We also show that the critical behavior can be extracted via a simple numerical algorithm, which we discuss in some detail in the Appendix.

The following sections are devoted to investigating exact analytic results in the infinite (dimensionless) spin-spin cou-

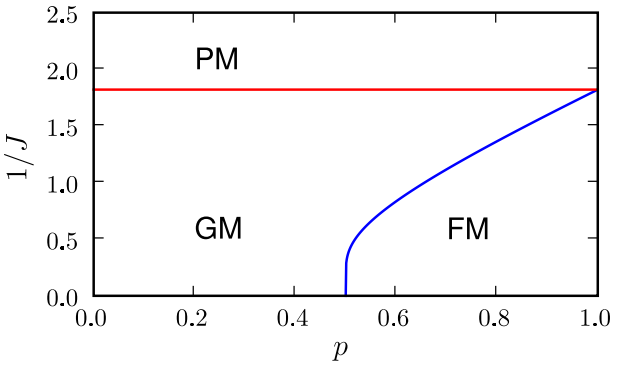

FIG. 1. (Color online) Phase diagram for the diluted ferromagnet on the connectivity $q=3$ Bethe lattice. The model is paramagnetic (PM) for any coupling weaker than J_G. It is ferromagnetic (FM) above the percolation transition ($p_c=1/2$) for strong enough couplings $J_c(p)\geqslant J_G$ and there are essential singularities but no spontaneous magnetization throughout the Griffiths-McCoy region (GM).

pling limit, $J=\infty$. This corresponds to the horizontal axis of the phase diagram in Fig. 1. In Sec. IV, we find an explicit expression for the magnetization $M(H)$ by means of a sum over connected clusters, which follows the standard GM treatment due to [16]. In Sec. V we show that the same expression can, in fact, be extracted from the cavity method. In this limit, the magnetization goes to zero with the field for $p\leqslant p_c=1/(q-1)$ while for $p>p_c$ a spontaneous magnetization develops. We first show that: (i) for $p<p_c$ the asymptotic series expansion for the magnetization contains only integer powers $M(H)=\chi H+c_3H^3+\ldots$, and (ii) on the contrary at $p=p_c$ the series expansion contains semi-integer powers as well $M(H)=c_{1/2}\sqrt{H}+c_1H+c_{3/2}H^{3/2}+\ldots$. That is, the critical exponent $\delta=2$ at $p=p_c$, $J=\infty$.

In Sec. VI we develop an alternative integral representation for $M(H)$ that corresponds to a harmonic expansion. This representation will allow us to calculate the (smoothed) density of Lee-Yang (LY) zeros ρ_{sm} at $J=\infty$ on the imaginary H axis ($\theta=\mathrm{Im}\,H$) in Sec. VII and to show that for $p<p_c$ a GM phenomenon indeed occurs, i.e., the density of zeros is nonzero and vanishes as $e^{-\alpha/\theta}$ when approaching the origin. For $p=p_c$ we find $\alpha=0$ and the density vanishes as the power law $\rho\propto\sqrt{\theta}$.

Finally, the promised Appendix briefly describes the "population dynamics" algorithm used in the numerical work.

III. PHASE DIAGRAM AND CAVITY EQUATIONS

The p-J phase diagram (Fig. 1) of the diluted ferromagnet $\mathcal{H}_\epsilon$ is physically well understood and can be derived naturally in a cavity method formalism [17,18]. In this approach, one considers the flow of cavity fields from the boundaries of the tree inward toward the center. A *cavity field* h_i on a spin σ_i at a distance d from the boundary describes the spin's magnetization in the absence of the link connecting it to the next spin inward. The cavity field h_i only depends on the cavity fields on σ_i's neighbors at distance $d-1$ and therefore one can define a natural flow for the depth dependent distribution of fields $P^{(d)}(h)$:

$$P^{(d)}(h)=\mathbb{E}_\epsilon\int\left(\prod_{i=1}^{q-1}dh_iP^{(d-1)}(h_i)\right)\delta\left(h-\sum_{i=1}^{q-1}u(h_i+H,J\epsilon_i)\right), \tag{2}$$

where

$$u(h_i+H,J\epsilon_i)=\tanh^{-1}(\tanh(J\epsilon_i)\tanh(h_i+H)) \tag{3}$$

gives the bias on the field h due to a spin σ_i connected through a link $J\epsilon_i$. $\mathbb{E}_\epsilon$ is the expectation with respect to the ϵ_{ij} distribution. Fixed point distributions $P^{(\infty)}(h)$ describe the statistical features of the bulk (central region) of the Bethe lattice. In order to break the Ising symmetry, we will always assume an infinitesimal uniform positive boundary field $P^{(0)}(h)=\delta(h-0^+)$ as the starting point for the flow.

In the undiluted model, $p=1$, all of this discussion reduces to the simple Bethe-Peierls mean field theory for a connectivity q lattice. Since there is no randomness, the cavity field distributions $P^{(d)}$ are simply delta functions located at, possibly depth dependent, fields $h^{(d)}$. Equation (2) reduces to a flow equation for $h^{(d)}$:

$$\begin{aligned}h^{(d)}&=\sum_{i=1}^{q-1}u(h^{(d-1)}+H,J)\\&=(q-1)\tanh^{-1}(\tanh(J)\tanh(h^{(d-1)}+H)).\end{aligned} \tag{4}$$

For $J<J_G=\tanh^{-1}(\frac{1}{q-1})$, the flow at $H=0$ has only one fixed point $h^{(\infty)}=0$ corresponding to the paramagnetic phase. For $J>J_G$, the $h^{(\infty)}=0$ fixed point becomes unstable to a spontaneously magnetized ferromagnetic fixed point with $h^{(\infty)}>0$. Expansion of the fixed point equation to leading order in H and $\epsilon=(J-J_G)$ gives the well-known mean-field critical exponents at $J=J_G$:

$$\begin{aligned}&M(H,J=J_G)\sim H^{1/\delta};\quad \delta=3\\&M(H=0,J>J_G)\sim(J-J_G)^\beta;\quad \beta=1/2.\end{aligned} \tag{5}$$

Under dilution, we must return to the more general cavity distribution flow defined by equation (2) to extract the phase behavior. Notice that the paramagnetic cavity distribution $P^{PM}(h)=\delta(h)$ is always a fixed point of the flow at $H=0$, just like $h^{(d)}=0$ is always a solution for the undiluted model. As in undiluted case, this fixed point will become unstable above some critical coupling $J_c(p)$. Near $P^{PM}(h)$ (i.e., for small h), we consider the linear stability of the first moment of $P^{(d)}(h)$:

$$\begin{aligned}\langle h\rangle^{(d)}&=\mathbb{E}_\epsilon\int dh\left(\prod_{i=1}^{q-1}dh_iP^{(d-1)}(h_i)\right)\delta\left(h-\sum_{i=1}^{q-1}u_i\right)h\\&=E_\epsilon\int\left(\prod_{i=1}^{q-1}dh_iP^{(d-1)}(h_i)\right)\sum_{i=1}^{q-1}u(h_i,J\epsilon_i)\\&\approx(q-1)(\mathbb{E}_\epsilon\tanh(J\epsilon))\langle h\rangle^{(d-1)},\end{aligned}$$

to leading order. Thus, $1=(q-1)p\,\tanh(J_c(p))$ gives the critical boundary separating a stable paramagnetic phase from

the ferromagnetic phase. A small rearrangement gives

$$J_c(p) = \tanh^{-1}\left(\frac{p_c}{p}\right). \tag{6}$$

This agrees precisely with the undiluted critical point $J_c(p=1)=J_G$ found above and also predicts that for $p<p_c$ the paramagnetic phase persists for all finite J. There is no ferromagnetic phase transition for a model with only finite clusters, as one expects.

In order to extract the critical behavior along the diluted phase boundary, we wish to expand the fixed point equations near the critical solution as we did in the discussion of the undiluted model. Rather than working with Eq. (2) directly, it is more natural to use an equivalent infinite set of recursion relations for the moments of $P(h)$. These can be derived by multiplying both sides of Eq. (2) by h^n and integrating or by considering the relation on random variables

$$h'^{(d)} = \sum_{i=1}^{q-1} \epsilon_i \tanh^{-1}(\tanh(J)\tanh(h_i^{(d-1)}))$$

taken to the power n and averaged. Near $P^{PM}(h)$, we expand this relation around small h_i:

$$h' = \sum_{i=1}^{q-1} \epsilon_i \tau\left(h_i - \frac{1}{3}(1-\tau^2)h_i^3\right) + \cdots, \tag{7}$$

where $\tau=\tanh J$ and we have suppressed the depth superscripts.

Sufficiently near the phase boundary, we expect the moments $\langle h^n\rangle$ to decrease exponentially with n and thus only a few leading order moments need be retained to extract the leading critical behavior at finite J. Taking powers of Eq. (7) and averaging, we find

$$\langle h'\rangle = 2p\tau\langle h\rangle - \frac{2}{3}p\tau(1-\tau^2)\langle h^3\rangle,$$

$$\langle h'^2\rangle = 2p\tau^2\langle h^2\rangle + 2p^2\tau^2\langle h\rangle^2,$$

$$\langle h'^3\rangle = 2p\tau^3\langle h^3\rangle + 6p^2\tau^3\langle h\rangle\langle h^2\rangle,$$

to cubic order. We have specialized to the case $q=3$ in order to simplify the presentation; for $q>3$ an additional term at cubic order is generated but the critical exponents remain the same.

Near the phase boundary in the p-J plane, we can define a small parameter ϵ by writing $2p\tau=\frac{p}{p_c}\tanh J=1+\epsilon$. We will treat the fixed point equations to leading order in the ϵ expansion. For $\epsilon<0$ the only real solution is paramagnetic:

$$\langle h\rangle = \langle h^2\rangle = \langle h^3\rangle = 0. \tag{8}$$

This solution is stable since its local Lyapunov exponents $(\epsilon, \epsilon-\ln\frac{1}{\tau}, \epsilon-2\ln\frac{1}{\tau})$ are all negative.

For $\epsilon>0$ this solution becomes unstable. We find two other ferromagnetically ordered solutions, which are linked by the symmetry $h\to -h$, and choose the positive one. This is

$$\langle h\rangle = 2\sqrt{\frac{1-\tau}{\tau}}\epsilon^{1/2} + \cdots,$$

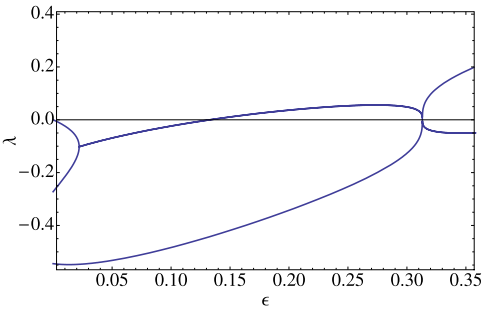

FIG. 2. (Color online) Lyapunov exponents of the ferromagnetic fixed point of the iteration equations for $J=1$. Notice that for $\epsilon<0.13\ldots$ they are all negative, signaling stability of the solution. At larger ϵ, the stationary point becomes a focus before eventually becoming unstable.

$$\langle h^2\rangle = \frac{2}{\tau}\epsilon + \cdots,$$

$$\langle h^3\rangle = \frac{6}{\sqrt{\tau(1-\tau)}}\frac{\epsilon^{3/2}}{1+\tau} + \cdots. \tag{9}$$

One can find the Lyapunov exponents of this stationary point analytically but the expressions are unenlightening. We plot a typical case in Fig. 2. Notice that the results (9) are consistent with the assumption that $\langle h^n\rangle$ decreases exponentially with n.

From Eq. (9) one can read off the critical exponent $\beta=1/2$ as the power of ϵ in $\langle h\rangle\sim m$. This is valid for all $\tau<1$ and sufficiently small ϵ. The point $\tau=1$ $(J=\infty)$ is different and needs to be treated more carefully. As $\tau\to 1$ the coefficient of $\epsilon^{1/2}$ in Eq. (9) vanishes, which implies that the $J=\infty$ critical exponent $\beta'>1/2$ while the divergence of the coefficient of $\epsilon^{3/2}$ means that $\beta'<3/2$. Indeed, from the exact solution of Sec. IV, we will find $\beta'=1$.

For sufficiently large $\epsilon>\epsilon_c$, the Lyapunov exponents become positive, signaling a loss of stability of the third order ferromagnetic solution [for the value $J=1$, $\tau=\tanh(1)$ in Fig. 2, $\epsilon_c=0.137\ldots$]. This indicates that the first few moments flow to large scale and our truncation to cubic order fails. The value of ϵ_c decreases monotonically as τ approaches 1 and to accurately find the fixed points we need to keep track of more moments of h in our iteration equations. At this point it is convenient to switch to numerical solution of the full cavity equation (2) by population dynamics, as described in the Appendix.

Having explored both above and below the critical point, we return briefly to the critical point at $\epsilon=0$. Here, at linear order, there is a marginal flow near the paramagnetic fixed point. It is possible to analyze the truncated flow equations (8) at higher order to discover that the paramagnetic solution is indeed algebraically (rather than exponentially) stable, as one expects of a second order phase transition. With some additional algebra it is possible to carry a small applied field H through all of the above arguments at $\epsilon=0$ and show that the critical exponent $\delta=3$ all along the $p>p_c$ phase boundary.

The final important feature of the phase diagram is the presence of GM singularities throughout the $p<1$, $J>J_G$ region. That is, the density of LY zeros on the imaginary H axis of the partition function has an essential singularity like $e^{-a'/\mathrm{Im}\,H}$ throughout this region due to the cumulative influence of rare large undiluted regions and there is therefore no gap. Equivalently, the real magnetization $M\sim e^{-a/H}$ in a real applied field H. Although this can be seen from elementary rigorous arguments [7,8], it is difficult to detect either analytically or numerically at finite J. However in Secs. VI and VII we will use the exact solution of the cavity equations at $J=\infty$ to exhibit these essential singularities explicitly and subject them to detailed study.

IV. CLUSTER SERIES AT $J=\infty$

For the remainder of the paper, we will focus primarily on the $J=\infty$ part, of the phase diagram of the model. We first review the classic argument due to Harris [16] based on an expansion over connected clusters. This will lead to an exact series expansion for $M(H)$ that we will independently rederive using the cavity approach in Sec. V.

Consider a cluster of $n+1$ spins connected by n bonds. For $J\gg H\sim 1$ (which is the meaning of the $J=\infty$ limit) each connected cluster behaves like a piece of ferromagnet. Indeed for $H=0$ there are two degenerate ground states, one with all spins pointing up and one with all spins pointing down. The first excited states are spin flips at energy $\sim J$ above the ground states and their presence is negligible. Turning on a magnetic field H the degeneracy is broken and (if H is positive, say) the state with all spins pointing up is energetically preferred. Therefore the cluster will acquire a small magnetization:

$$M_n(H) = (n+1)\tanh((n+1)H). \tag{10}$$

The total magnetization per spin is obtained by summing over all the clusters with their weights W_n, corresponding to the number of clusters of size n per spin [19]

$$M(H) = \sum_{n\geqslant 0} W_n M_n(H). \tag{11}$$

This equation has been studied before and results can be found in [16] for the magnetization, and [20] for the scaling law of the magnetization at the critical point. We will reproduce those results on the magnetization for completeness, but the main focus of this paper will be the density of Lee-Yang zeros and the solution of cavity field equations from which we will recover the known results.

From the solution of the bond percolation problem on the Bethe lattice [15] the number per spin W_n of clusters of bond size n is given by

$$W_n(p) = q\frac{((n+1)(q-1))!}{(n+1)!(n(q-2)+q)!}p^n(1-p)^{n(q-2)+q}.$$

For simplicity, we consider $q=3$ in the following as all of the essential physics are already present. We can easily obtain the asymptotic behavior of the magnetization by using the asymptotics of W_n as

$$W_n \sim \frac{12}{\sqrt{\pi}}(1-p)^3\left(\frac{1}{n}\right)^{5/2} e^{-nA(p)}, \tag{12}$$

where

$$A(p) = \ln\frac{1}{4p(1-p)}. \tag{13}$$

$A(p)$ is the exponent governing the decay rate of the cluster sizes and it will appear often in the remainder of the paper. For $p<p_c=1/2$, $A>0$ and W_n decreases exponentially. For $p=p_c$, $A=0$ and we have instead a power-law decay with exponent $5/2$ (the exponent is independent of q):

$$W_n \sim \frac{3}{2\sqrt{\pi}}\left(\frac{1}{n}\right)^{5/2}. \tag{14}$$

This change in the asymptotic fall off of the cluster distribution at criticality is the reason for the change in the response to an applied external field at zero temperature.

Indeed we can easily see how this works. For $A>0$ and small H we can write an asymptotic expansion by expanding the tanh in the sum (11):

$$\begin{aligned} M(H) &= \sum_n W_n(n+1)\tanh((n+1)H) \\ &\simeq H\langle(n+1)^2\rangle + \mathcal{O}(H^3) \\ &= H\frac{1+p}{1-2p} + \mathcal{O}(H^3), \end{aligned} \tag{15}$$

which is linear in H. *At* the percolation threshold, however, $A=0$ and $\langle n^2\rangle$ diverges. The expansion of tanh inside the first sum is unjustified. To find the first term in the asymptotic expansion of M (that we will derive in a formally correct way in Sec. VI) we use instead Eq. (12):

$$\begin{aligned} M(H) &\simeq \sum_n \frac{3}{2\sqrt{\pi}}\left(\frac{1}{n}\right)^{3/2}\tanh(nH) \\ &\simeq \frac{3}{2\sqrt{\pi}}\sqrt{H}\int_0^\infty dx x^{-3/2}\tanh x + \mathcal{O}(H). \end{aligned} \tag{16}$$

So the susceptibility diverges although there is no spontaneous magnetization [16]. We now turn to a derivation of the above results from the cavity method.

V. CAVITY APPROACH AT $J=\infty$

The cavity method for this system gives a probability distribution for the cavity fields which satisfies the fixed point equation [cf. Eq. (2)],

$$P(h) = \mathbb{E}_\epsilon \int \prod_{i=1}^{q-1} dh_i P(h_i)\delta\left(h - \sum_{i=1}^{q-1} u(h_i+H,J\epsilon_i)\right). \tag{17}$$

In the $J\to\infty$ limit, we can linearize the cavity biases u:

$$u(h+H,J\epsilon_i) = (h+H)\epsilon_i. \tag{18}$$

At $q=3$, the fixed-point equation (17) becomes

$$P(h) = (1-p)^2\delta(h) + 2p(1-p)P(h-H) + p^2\int dh_2 P(h_2-2H)P(h-h_2).$$

This equation can be solved by defining the Laplace transform

$$g(s) = \int_{0^-}^{\infty} dh P(h) e^{-sh},$$

making sure to include the delta function at $h=0$. The equation for g is quadratic

$$0 = p^2 e^{-2sH} g(s)^2 + (2p(1-p)e^{-sH} - 1)g(s) + (1-p)^2, \tag{19}$$

with solution

$$g(s) = \frac{e^{2Hs} - 2e^{Hs}(p-p^2) - e^{3Hs/2}\sqrt{e^{Hs} - 4(p-p^2)}}{(2p^2)}. \tag{20}$$

The second solution to Eq. (19) is not physical. Even without inverting the Laplace transform all the properties of the solution can be extracted from $g(s)$. For example the normalization condition, the zeroth moment, is

$$\int_0^{\infty} dh P(h) = g(0) = \begin{cases} 1 & \text{if } p \leqslant 1/2 \\ \dfrac{(1-p)^2}{p^2} & \text{if } p > 1/2, \end{cases}$$

and the first moment is

$$\langle h \rangle = -\left.\frac{\partial g}{\partial s}\right|_{s=0} = \frac{2Hp}{1-2p} \tag{21}$$

whose divergence at $p=p_c=1/2$ signals the ferromagnetic phase transition. For $p>p_c$, $P(h)$ loses normalization because a finite fraction of the cavity fields flow to infinity, just as in a percolating cluster distribution. Indeed, the divergent cavity fields are precisely those attached to spins in percolating clusters. Because these spins are connected to the positively biased boundary and the temperature is effectively zero, they spontaneously magnetize to $M=1=\tanh(\infty)$. This provides the spontaneous magnetization critical exponent:

$$M(H=0, J=\infty, p) = 1 - \frac{(1-p)^2}{p^2} \propto (p-p_c)^1$$

from which we read $\beta'=1$ in accord with the discussion following Eq. (9).

We now concentrate on the $p \leqslant p_c = 1/2$ region at finite H. Consider the magnetization per spin

$$M(H) = \left\langle \tanh\left(H + \sum_{i=1}^{q} u(h_i + H, J\epsilon_i) \right) \right\rangle_{\epsilon, h_i}, \tag{22}$$

which is obtained by averaging over the disorder and the distribution of h. It is straightforward to show that for small h and H we obtain the results of Eq. (15). Indeed:

$$M(H) = \left\langle H + \sum_{i=1}^{q} \epsilon_i (h_i + H) \right\rangle_{\epsilon, h} + \mathcal{O}(H^3) \tag{23}$$

$$= (1+3p)H + 3p\langle h \rangle + \mathcal{O}(H^3). \tag{24}$$

Now substitute Eq. (21) and simplify

$$M(H) = H\frac{(1+p)}{1-2p} + \mathcal{O}(H^3), \tag{25}$$

in accordance with Eq. (15).

We now reconstruct the full probability distribution $P(h)$ exactly. We expand the function $g(s)$ as a series in e^{-sH}

$$g(s) = \sum_{n \geqslant 0} \alpha_n e^{-snH} \tag{26}$$

which defines the coefficients α_n. $P(h)$ is now given by the inverse Laplace transform,

$$P(h) = \sum_{n \geqslant 0} \alpha_n \delta(h - nH). \tag{27}$$

The α_n are given by the series expansion of the square root in Eq. (20):

$$\alpha_n = \frac{(4p(1-p))^{n+2}}{2p^2} \frac{(-1)^{n+1}\Gamma(3/2)}{\Gamma(n+3)\Gamma(-n-1/2)}. \tag{28}$$

That is, $P(h)$ is a comb of delta functions at integer multiples of H with a decaying envelope. The large n behavior of the envelope is

$$\alpha_n = \frac{4(1-p)^2}{\sqrt{\pi}} n^{-3/2} e^{-A(p)n} + \ldots, \tag{29}$$

where $A(p)$ is defined in Eq. (13). It is not surprising that the same asymptotics governs both $P(h)$ and W_n.

Finally, to connect directly with the previous section let us compute the exact magnetization of a spin as a function of applied field H. Evaluating the cavity magnetization equation (22) using the cavity field distribution (27), we find

$$M(H) = \sum_{j=0}^{q} \binom{q}{j} p^j (1-p)^{q-j} \sum_{m_1, \cdots, m_j = 0}^{\infty} \alpha_{m_1} \cdots \alpha_{m_j} \tanh((j + 1 + m_1 + \cdots + m_j)H) \tag{30}$$

which naturally expands as a series in $\tanh nH$. At $q=3$, we can evaluate all the coefficients in this series to find that indeed they are identical to the coefficients nW_{n-1} of Eq. (11). Thus, at $J=\infty$ the cluster series and the cavity method produce identical results for the magnetization.

Having established the equivalence of the two solutions, we now return to the analysis of the series for the magnetization. In the following two sections we will extract the critical behavior near $p=p_c$ and, by analytic continuation to imaginary H, the GM singularity in the density of LY zeros.

VI. AN INTEGRAL REPRESENTATION FOR THE MAGNETIZATION

Despite its simplicity, the expansion of Eq. (11) is an exact result for the magnetization which can be analytically

continued to imaginary values of the magnetic field. However, the representation of $M(H)$ as a sum in Eq. (11) is not best suited for this purpose. An integral representation would be preferable. To obtain it we write the Laplace transform of the function $\tanh x$

$$f(s) = \int_0^\infty dx e^{-sx} \tanh x = \frac{1}{2}\left(-\frac{2}{s} - \psi\left(\frac{s}{4}\right) + \psi\left(\frac{2+s}{4}\right)\right), \tag{31}$$

where ψ is the digamma function. The function $f(s)$ has simple poles only at the negative even integers and thus we can invert the transform and write

$$\tanh x = \int_B \frac{ds}{2\pi i} e^{sx} f(s), \tag{32}$$

where B is any Bromwich path lying to the right of all poles of $f(s)$, that is to the right of the negative real axis. Inserting into Eq. (11), we can invert sum and integral, provided

$$|4p(1-p)e^{sH}| < 1. \tag{33}$$

The resulting expression, valid for $|\arg H| < \pi/2$,

$$M(H) = 3(1-p)^3 \int_B \frac{ds}{2\pi i} f(s) \sum_{n\geq 0} \frac{2(n+1)!}{(n+3)!n!} e^{s(n+1)H} \times (p(1-p))^n$$

can be written in closed form by performing the sum. This amounts to calculating the derivative of the generating function of the probability W_n. For the Bethe lattice the generating function is [21]

$$\phi(x) = \sum_{n\geq 0} W_n x^n = -2(1-p)^3 x^{-3}(8(1-\sqrt{1-\xi}) + 4(2\sqrt{1-\xi}-3)\xi + 3\xi^2), \tag{34}$$

where $\xi = 4p(1-p)x$ has been defined for convenience. By means of this function we can perform the sum inside the integral to obtain

$$M(H) = \frac{3(1-p)^3}{6p^3(1-p)^3} \int_B \frac{ds}{2i\pi} f(s) e^{-2sH} \{[p(1-p)e^{sH} - 1] \times \sqrt{1-4p(1-p)e^{sH}} + 1 - 3p(1-p)e^{sH}\}. \tag{35}$$

We simplify this expression by considering the analytic structure of the integrand (see Fig. 3). The function $f(s)$ has simple poles at the non-positive even integers $(0,-2,-4,\ldots)$, while the rational expression has a series of square root cuts at $s_n^* = \frac{A(p)}{H} + i2\pi n/H$. We close the contour with a semicircle at infinity on the right (for $\mathrm{Re}\, s > 0$) on the first Riemann sheet. We then deform the contour to coincide with the edges of the cuts. At this point only the discontinuity across the cuts contributes to the final result. For aesthetic reasons we finally shift the value of s by $\frac{A(p)}{H}$, the real part of the origins of the cuts.

The resulting expression is

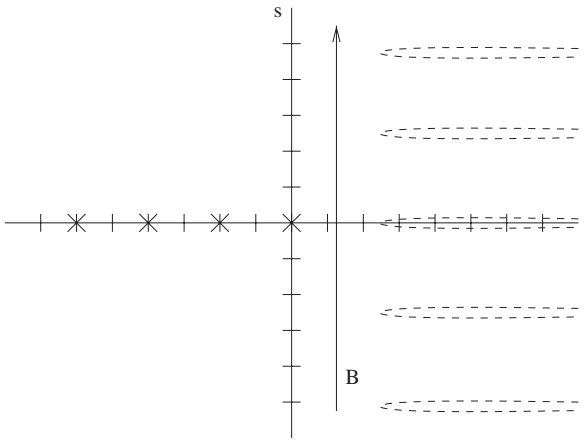

FIG. 3. Analytic structure of integrand of Eq. (35). The function $f(s)$ has simple poles at nonpositive even integers while the rational expression has square root cuts at $s_n^* = \frac{A(p)+2\pi in}{H}$ which we connect to infinity at the right. B labels the undeformed Bromwich path.

$$M(H) = \frac{8(1-p)^2}{\pi p} \sum_{n=-\infty}^{\infty} \int_0^\infty ds f(s + s_n^*) \times e^{-2sH}\left(1 - \frac{1}{4}e^{sH}\right)\sqrt{e^{eH}-1}. \tag{36}$$

At this point it seems we have traded a sum of functions (16) with a series of integrals that we cannot evaluate. This looks like a step backward in the quest for a useful result. However, after thinking about the procedure we have performed, we recognize that this is a Poisson summation like duality on the original equation (11). The terms in the sum are higher and higher harmonics of the result (this is particularly evident, as we will see shortly, for imaginary H).

The series in n in Eq. (36) is dual to the series in Eq. (11) so that when the first converges rapidly the second does not and vice versa (for H on the real axis). In the interesting regime, close to the percolation threshold (11) converges slowly and the first term $(n=0)$ of Eq. (36) gives the leading term in the expansion in $(p-p_c)$ and $H \to 0$.

Let us now see how we can recover Eq. (16) in a clean way. At the critical point $p=1/2$, we have $A=0$ and so $s_n^* = i2\pi n/H$. For $H \to 0$ all the cuts except that corresponding to $n=0$ go to infinity and we can keep only the $n=0$ term in the series (36). Moreover, by expanding the integrand in powers of H we find

$$M(H) \simeq \frac{3}{\pi}\sqrt{H}\int_0^\infty ds \sqrt{s} f(s) + \mathcal{O}(H) = \frac{3}{\pi}\sqrt{H}\frac{\sqrt{\pi}}{2}\int_0^\infty dx\, x^{-3/2} \tanh x + \mathcal{O}(H)$$

which coincides with Eq. (16).

To recapitulate, the magnetization is given by an integral of the *discontinuous part* of the generating function ϕ of the cluster distribution W_n with the Laplace transform of the function $\tanh x$. For the Bethe lattice the generating function can be written explicitly and the calculations can be carried

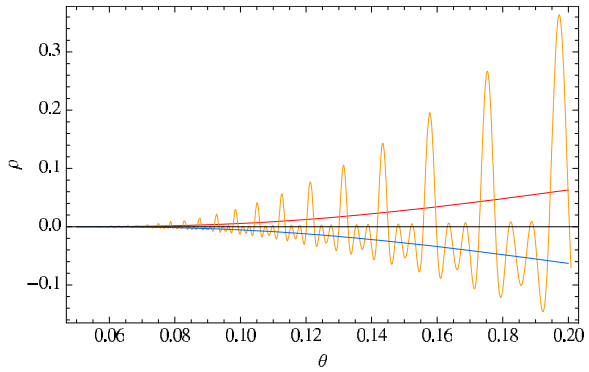

FIG. 4. (Color online) The density of Lee-Yang zeros as a function of the imaginary field θ at $p=1/4$. The upward bending smooth curve (red) is the smoothed ρ_{sm}; the oscillatory curve (orange) is the sum of the first three harmonics in Eq. (36) (terms $n=\pm1,\pm2,\pm3$) and the downward bending smooth curve (blue) is $-\rho_{sm}$. The figure suggests (in agreement with the discussion in the text) that the sum of all the harmonics (with $n\neq0$) builds a sum of delta functions Eq. (37) *minus* ρ_{sm} in Eq. (40).

to the end. In the percolation limit the cut on the real axis gives the greatest contribution to the sum.

VII. DENSITY OF LEE-YANG ZEROS AT $J=\infty$

In this section we will find the density of Lee-Yang zeros ρ at $J=\infty$. These are the zeros of the partition function as a function of the external magnetic field H, for imaginary $H=i\theta$. Instead of solving the equation $Z(H)=0$ directly, we rely on the relation [13]

$$\rho(\theta)=\frac{1}{\pi}\,\mathrm{Re}\,M(i\theta+0^+).$$

To get an idea of how this function looks we recall

$$\mathrm{Re}\tanh(i\theta+0^+)=\pi\sum_{m=-\infty}^{\infty}\delta\left(\theta-\frac{\pi}{2}(2m+1)\right).$$

Substituting this into Eq. (15), we find

$$\rho(\theta)=\sum_m\sum_{n\geqslant0}W_n(n+1)\delta\left((n+1)\theta-\frac{\pi}{2}(2m+1)\right)$$
$$=\sum_{m,n}W_n\delta\left(\theta-\pi\frac{2m+1}{2n+2}\right),\tag{37}$$

so the zeros are located at all the $\frac{\text{odd}}{\text{even}}$ rational multiples of π, with multiplicities given by the W_n's [22]. This is a singular distribution with an accumulation point at $\theta=0$: our task is now to smooth it by using the Poisson-dual integral representation (36) obtained in the previous section.

For imaginary H, the expansion over the cuts becomes an harmonic expansion (see Fig. 4) of ρ. Selecting the term with $n=0$ in Eq. (36), gives the function smoothed to the lowest degree:

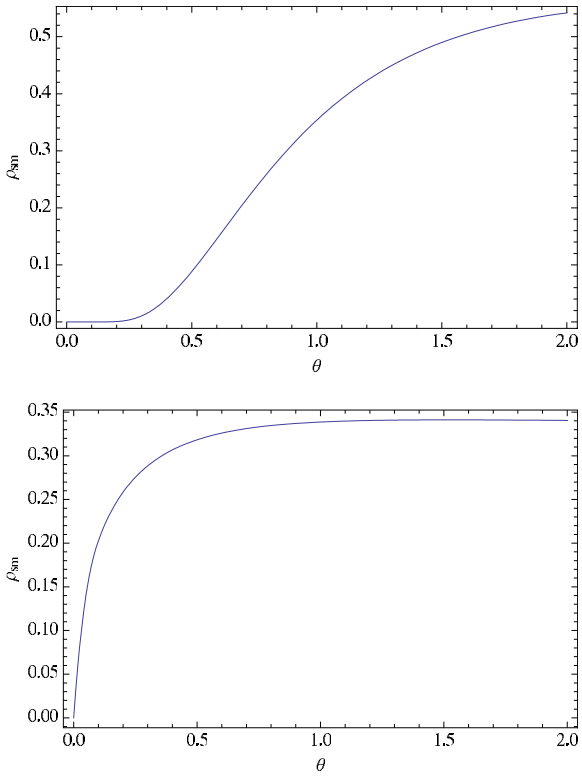

FIG. 5. (Color online) The density of Lee-Yang zeros as a function of the imaginary field θ at $p=1/10$ (above) and at criticality $p=1/2$ (below).

$$\rho_{\mathrm{sm}}(\theta)=\frac{8(1-p)^2}{\pi^2p}\int_0^\infty ds\sqrt{e^{s\theta}-1}\left(1-\frac{1}{4}e^{s\theta}\right)e^{-2s\theta}$$
$$\times\,\mathrm{Im}\,f(-is-iA(p)/\theta+0^+).\tag{38}$$

This expression simplifies since from the definition of f

$$\mathrm{Im}\,f(-iz+0^+)=\int_0^\infty dx\,\sin(zx)\tanh x=\frac{\pi}{2\sinh\pi z/2}.\tag{39}$$

So we find the smoothed density of LY zeros

$$\rho_{\mathrm{sm}}(\theta)=\frac{4(1-p)^2}{\pi p}\int_0^\infty ds\sqrt{e^{s\theta}-1}\left(1-\frac{1}{4}e^{s\theta}\right)$$
$$\times\frac{e^{-2s\theta}}{\sinh\left(\frac{\pi}{2}(s+A\theta)\right)}.\tag{40}$$

The different profiles for this density can be seen in Fig. 5. Here the GM phenomenon is evident: even at $p<p_c=1/2$, $\rho_{\mathrm{sm}}(\theta)$ is strictly positive for any nonzero θ; there is no gap in the distribution. This effect is due to the presence of rare large clusters. The asymptotic expansion of the density at small θ can be found by expanding the integrand to leading order in θ:

$$\rho(\theta) \simeq \frac{4(1-p)^2}{\pi p}\int_0^\infty ds\sqrt{s\theta}\left(\frac{3}{4}\right)\frac{1}{\frac{1}{2}e^{(\pi/2)s}e^{(\pi/2)A/\theta}}$$

$$\simeq \frac{3\sqrt{2}(1-p)^2}{4\pi^2 p}\sqrt{\theta}e^{-(\pi/2)A/\theta}. \quad (41)$$

This expansion is uniformly valid at the point $A=0$, which is $p=p_c$, where it shows the critical square root cusp in the magnetization. However, let us remark that Eq. (40) is the smoothed part (in the sense of distributions) for all values of θ and not only for small θ.

Let us now make a few qualitative remarks on the asymptotic expansions for $M(H)$ and ρ which apply in principle to all lattices. From the integral representation (35) (see Fig. 3) we observe that there is no Stokes phenomenon for Re $H>0$. That is, the asymptotic approximation for $M(H)$, Eq. (15) to higher order,

$$M_L(H) = \sum_{k=0}^{L} a_k H^{2k+1}\langle (n+1)^{2k+2}\rangle + \mathcal{O}(H^{2L+1}) \quad (42)$$

(where a_k's are the coefficients in the series expansion for $\tanh x$) is valid for all $|\arg H|<\pi/2$.

Naively, substituting $H=i\theta+0^+$ term by term into this expansion, we obtain a purely imaginary result for any L. Since $M_L(H)$ is odd, we might speculate that $\rho=0$. However, the expansion (42) is only asymptotic, since $\langle (n+1)^k\rangle \sim k!e^{-k\mathcal{A}}$. This means that we cannot take $L\to\infty$ but must instead truncate the series at the $L\sim H/\mathcal{A}$ where the remainder is smallest. The remainder is never actually zero but it is exponentially small in $1/|H|$. A good quantitave approximation can be found by using the "terminant"[23] of the asymptotic expansion. The terminant is indeed $\propto e^{-\mathcal{A}/|H|}$ and *it is not* purely imaginary for $H=i\theta+0^+$. Thus, as a general rule we expect the real part of the terminant of the asymptotic expansion of $M(H)$ represents the density of LY zeros in the subcritical region.

VIII. SUMMARY

The diluted Ising ferromagnet on a Bethe lattice is a tractable model that beautifully illustrates many of the key physical features of short-ranged disordered systems. In this paper, we have attempted to present a unified analysis of the model in the framework of the cavity method, from which we derive both well-known elementary results about its phases and nontrivial features such as GM singularities and the infinite coupling critical exponents.

In particular, the ferromagnetic phase boundary lies in the mean-field universality class ($\delta=3$) at any dilution above the percolation threshold. At this threshold however, the ferromagnetic critical coupling diverges ($J\to\infty$) and our closed form solutions for the cavity distributions in this limit reveal that the critical behavior is governed by the percolation of the underlying lattice ($\delta=2$). Linear stability analysis of the flow of the cavity moments near criticality naturally reveals the Lyapunov exponents and the associated correlation depth of the stable phases.

Furthermore, at infinite coupling we have explicitly exhibited the essential Griffiths-McCoy singularities in the magnetization for all $p<p_c$, where there is no spontaneous magnetization. By an harmonic resummation of the exact magnetization, we found the smoothed density of LY zeros exactly and conjectured its relation to the real part of an appropriate terminant of the asymptotic series for the magnetization.

ACKNOWLEDGMENTS

The authors would like to thank M. Aizenmann for discussions and for catching an error in an earlier version of the draft. C.L. and A.S. would like to thank S. Franz and R. Zecchina for discussions and A. S. would like to thank G. Marmo for discussions and acknowledges support from the MECENAS program of the Universita' Federico II di Napoli, where part of this work was completed. C.L. acknowledges support from the NSF. The work of S.L.S. is supported by the NSF Grant No. DMR 0213706.

APPENDIX: NUMERICAL METHODS

In the cavity framework, all of the statistical observables of a model can be derived from the cavity field distribution $P(h)$. This distribution is the fixed point of the flow of the cavity equation (2). While we can solve this equation analytically in certain limits, we rely on a simple iterative numerical algorithm called *population dynamics* for many of the finite coupling results. Population dynamics and its more sophisticated variants appear in, for example, [24].

The algorithm works as follows: we represent the distribution $P(h)$ by a finite population of N_{pop} fields h_i. This population is initialized from an appropriate uniform distribution and then iterated as follows:

(i) Select $q-1$ fields h_i randomly from the population and $q-1$ random ϵ_{i0}.

(ii) Use Eq. (2) to calculate the cavity field h_0 on a spin sitting below the $q-1$ spins selected above.

(iii) Randomly replace one element of the population with h_0.

(iv) Repeat until convergence in some measure of the population, for example the cavity magnetization $\langle\tanh(h)\rangle$.

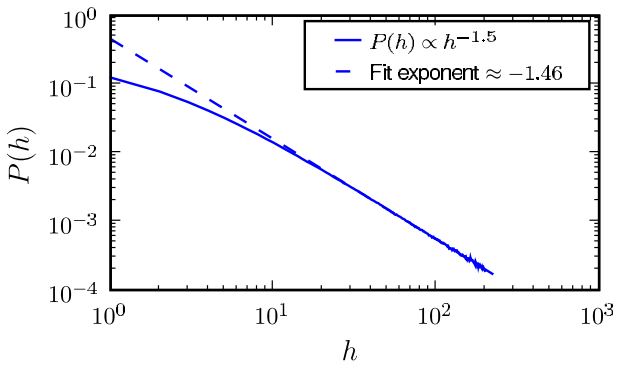

FIG. 6. (Color online) Cavity field distribution at $p=0.5$, $J=\infty$ critical point with $H=1$. This log-log plot shows agreement with the asymptotic form $P(h)\sim h^{-3/2}$ found in the exact solution.

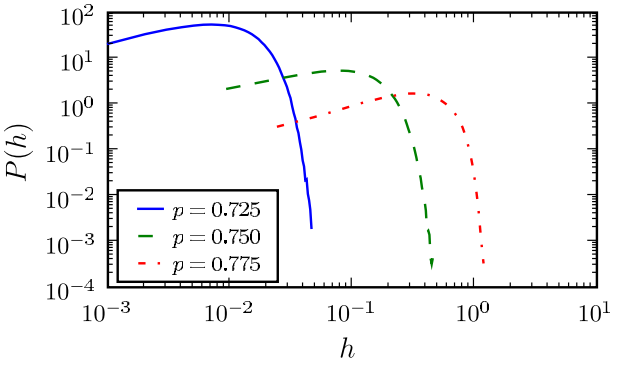

FIG. 7. (Color online) Cavity field distributions as function of p near the $p=0.75$, $J=0.80$ critical point at small applied field $H \approx 10^{-4}$. The solid (blue) curve is in the paramagnetic regime, the dashed (green) is in the critical phase and the dot dashed (red) in the ferromagnetic one. Notice the dramatic increase in the response of the cavity field distribution to the applied field on the ferromagnetic side of the phase boundary.

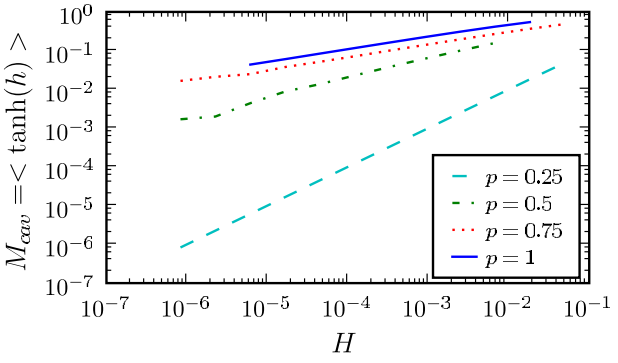

FIG. 8. (Color online) Critical magnetization in an external field along the $J=\infty$ line. The slope of the log-log curves indicates the critical exponent δ associated with each of the four points $p = 0.25, 0.5, 0.75, 1$ along the phase boundary. We find $\delta=1$ for $p = 0.25 < p_c = 0.5$, $\delta=2$ for $p=0.5$ and $\delta=3$ for $p=0.75$ and 1.

In practice, this procedure converges quickly, deep in either the ferromagnetic or paramagnetic phase, but slows near the phase transition. We illustrate some typical results below for $q=3$.

Even at the percolating critical point, when the expected cavity distribution develops a long tail and divergent moments, this procedure works. Figure 6 shows the numerically determined cavity field distribution for the $p=0.5$, $J=\infty$ critical point with applied field $H=1$. As noted in Sec. V, the exact solution is a comb of delta functions at $h=nH$, $n \in \mathbf{N}$ with weights decaying asymptotically as a power law $\alpha_n \sim n^{-3/2}$. The numerical solution concentrates on integer fields with a power-law tail consistent with the exponent -1.5.

In general, the form of the cavity field distribution at finite p and J is only obtainable numerically. Figure 7 shows the numerically determined distribution at small applied field H on three different points in the $p-J$ plane near the $p=0.75$, $J=0.80$ critical point. These distributions are typical and illustrate the dramatic increase in susceptibility on the ferromagnetic side of the phase boundary.

Finally, Fig. 8 confirms numerically the critical exponents derived using the moment flow analysis of Sec. III and the exact solution of Sec. IV.

[1] R. Baxter, *Exactly Solved Models in Statistical Mechanics* (Academic, London, 1982).

[2] NP stands for the class of nondeterministic polynomial algorithms. See for example M. Sipser, *Introduction to the Theory of Computation* (Course Technology, Boston, 1996).

[3] M. Mezard, G. Parisi, and R. Zecchina, Science **297**, 812 (2002).

[4] C. Laumann, A. Scardicchio, and S. L. Sondhi, Phys. Rev. B (to be published).

[5] M. B. Hastings, Phys. Rev. B **76**, 201102(R) (2007).

[6] D. Poulin and E. Bilgin, Phys. Rev. A **77**, 052318 (2008).

[7] R. Griffiths, Phys. Rev. Lett. **23**, 17 (1969).

[8] T. Vojta, J. Phys. A **39**, R143 (2006).

[9] B. McCoy and T. T. Wu, Phys. Rev. **176**, 631 (1968).

[10] For example, see the numerical work on the two-dimensional version of the problem studied in J. J. Ruiz-Lorenzo, J. Phys. A **30**, 485 (1997).

[11] V. S. Dotsenko, J. Phys. A **32**, 2949 (1999).

[12] V. Dotsenko, J. Stat. Phys. **122**, 197 (2006).

[13] A. J. Bray and D. Huifang, Phys. Rev. B **40**, 6980 (1989).

[14] J. Barata and D. Marchetti, J. Stat. Phys. **88**, 231 (1997).

[15] M. Fisher and J. Essam, J. Math. Phys. **2**, 609 (1961).

[16] A. Harris, Phys. Rev. B **12**, 203 (1975).

[17] J. S. Yedidia, W. T. Freeman, and Y. Weiss, Adv. Neural Inf. Process. Syst. **13**, 689 (2000).

[18] M. Mezard and G. Parisi, Eur. Phys. J. B **20**, 217 (2001).

[19] Notice that in this approach the infinite coupling limit is solvable because the magnetization of a cluster depends only on the number of spins in the cluster and not on its detailed shape.

[20] J. Essam, K. M. Gwilym, and J. Loveluck, J. Phys. C **9**, 365 (1976).

[21] The generating function can be derived for $q=4$ as well, while for generic q the result is written in terms of hypergeometric functions for which no explicit rational form seems to exist. We see below that the fundamental property of this generating function is to have a square-root branch cut at $\xi=1$. This exists for all $q>2$ due to a well-known property of the generalized hypergeometric functions.

[22] Usually, disorder averaging generates a smooth density of LY zeros, but not so in the infinite coupling limit of the diluted ferromagnet. This is because the thermodynamics only depend on the size of clusters and not their shape, and each cluster of size n contributes zeros precisely at odd multiples of $\pi/2n$.

[23] R. Dingle, *Asymptotic Expansions: Their Derivation and Interpretation* (Academic, London, 1973).

[24] M. Mezard and G. Parisi, J. Stat. Phys. **111**, 1 (2003).